

# **A Statistical Comparison of Vertical Total Electron Content (TEC) from Three Ionospheric Models**

*McArthur “Mack” Jones Jr.*

Academic Affiliation, Fall 2008: Senior, Millersville University

SOARS<sup>®</sup> Summer 2008

Science Research Mentor: Mihail Codrescu and Jennifer Gannon  
Writing and Communication Mentor: Marijke Unger

## **ABSTRACT**

[1] Total electron content (TEC) exhibits significant variations in both space and time depending upon latitude, longitude, solar cycle, UTC, and season; these variations can have potentially negative effects on communication and navigation systems. Recently, three models have provided accurate results in reconstructing and/or calculating real-time (or near real-time) vertical TEC values: the Utah State University Global Assimilation of Ionospheric Measurements (USU GAIM) Gauss-Markov Kalman Filter Model, the United States Total Electron Content (US-TEC) Model, and the Coupled Thermosphere Ionosphere Plasmasphere electrodynamics (CTIPE) Model. This research offers a statistical comparison of the vertical TEC outputs from the previously mentioned models on both a global and local (over the continental US) scale during the month of July 2008. We present the average difference and root mean square difference (RMS difference) for three different model comparisons (e.g. – US-TEC vs. GAIM, US-TEC vs. CTIPE, and GAIM vs. CTIPE). We have documented certain model biases and the differences measured between corresponding data points among the models relative to each comparison. Two out of the three comparisons showed that the US-TEC model’s bias predicted higher values of vertical TEC relative to the other models, while the third comparison revealed a small bias in the CTIPE model to forecast greater vertical TEC values when compared to the GAIM model. By computing the RMS difference, we can better examine the source of these biases relative to the aforementioned model comparisons. This is the first step in documenting the biases, errors, and uncertainties associated with these three models.

*The Significant Opportunities in Atmospheric Research and Science (SOARS) Program is managed by the University Corporation for Atmospheric Research (UCAR) with support from participating universities. SOARS is funded by the National Science Foundation, the National Oceanic and Atmospheric Administration (NOAA) Climate Program Office, the NOAA Oceans and Human Health Initiative, the Center for Multi-Scale Modeling of Atmospheric Processes at Colorado State University, and the Cooperative Institute for Research in Environmental Sciences. SOARS is a partner project with Research Experience in Solid Earth Science for Student (RESESS).*

## 1. Introduction

[2] For the last seventy years scientists have studied the Earth's ionosphere quite extensively through the use of multiple techniques (i.e., radiosounders, Faraday radars, top-side soundings from satellites, GPS signals, etc). Surprisingly, however, most people are unfamiliar with its existence, despite the fact that the ionosphere plays an integral role in many of their everyday activities. Extreme variations within the ionosphere induced by storm enhanced density (SED) events and responses to magnetic storms can adversely affect navigation and communication systems on Earth [Schunk *et al.*, 2004, Skone and Coster, 2008, Araujo-Pradere and Fuller-Rowell, 2002, Araujo-Pradere, *et al.*, 2002]. According to the *American Meteorological Society* [2000] the ionosphere is the upper region of the atmosphere that contains a significant concentration of charged particles, which affect the propagation of radio waves. When solar radiation strikes the atoms and molecules of the upper atmosphere, electrons are dislodged through the process of ionization. Because of the chemical composition of our atmosphere, the shorter wavelengths of solar radiation (the extreme ultraviolet and X-Rays) are energetic enough to ionize these atoms and molecules in the Earth's atmosphere [<http://www.swpc.noaa.gov/info/Iono.pdf>]. Depending on the energy of the incident photon, photoelectrons (i.e. - electrons emitted from an atom or molecule by an incident photon) are produced, with great enough energies to ionize other nearby neutrals or moleculars. Particle precipitation occurs when energetic particles are injected into the upper atmosphere and collide with neutrals. This process produces increased and variable levels of ionization [Bother and Dagleis, 2007]. In summary, highly variable production, loss, and conditional transport of ionization are responsible for the extremely variable ionosphere.

[3] Since the ionosphere is the result of a dynamic equilibrium between variable production, loss and transport processes, its vertical structure can be exceptionally complex and is typically divided into regions or layers (D, E, F), with each different layer referring to the ionization at some height. Additionally, a C layer can be present under specific ionospheric conditions. The amount of layers, their altitude, and their ionization densities vary significantly in time and space depending on latitude, longitude, universal time, solar cycle, season, and geomagnetic activity [Davies *et al.*, 1997]. The D-region, which is only present in the daytime and is produced only by the most energetic solar radiation impinging on Earth's upper atmosphere, is the lowest region in the ionosphere, extending from 50 – 90 km [Dabas, 2000]. The next layer is the E-region, which extends from 90 – 150 km; also located within the E-region are small-scale layers of variable ionization referred to as sporadic Es. E layers can scatter and or reflect radio waves to either improve or degrade radio communication (High Frequency communication) [Davies *et al.*, 1997]. The F-region is divided into two sub-layers (F1 and F2), and collectively these layers extend from 150 km to 600 km. The D and F regions of the ionosphere are of utmost importance to radio communication users because the D layer is responsible for the most radio wave attenuation (frequency range 3 MHz – 30 MHz, wavelength range 10 m – 100 m) and the F layer is used for reflecting incident radio waves [Dabas, 2000]. The top of the ionosphere is believed to be around 1000 km, although there is no definite boundary between the Earth's ionosphere, magnetosphere, and plasmasphere [<http://www.swpc.noaa.gov/info/Iono.pdf>]. One particular parameter associated with ionospheric structure is the total electron content (TEC), which is the integral value of the electron density along a path. Variable electron density levels can affect the

communication and navigation industries, which can lead to an array of problems [Goodman and Aarons, 1990].

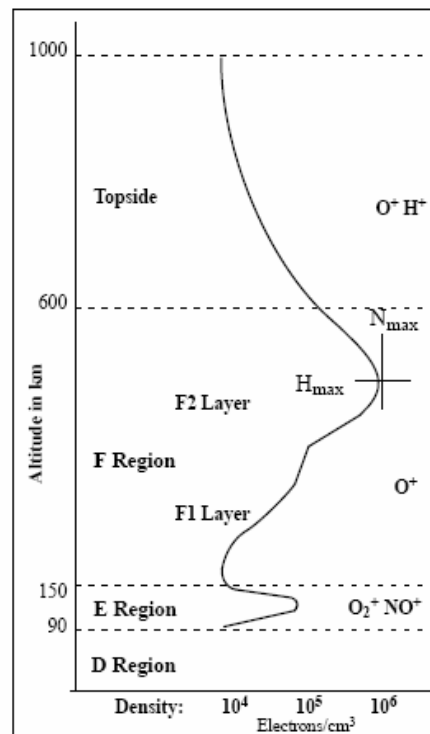


**Figure 1.** The different layers of the ionosphere and their predominant ions are displayed at their particular heights. The electron density profile is also displayed and it varies significantly with height. The above profile of electron density is shown for average conditions (i.e. daytime, mid-latitude, medium solar activity). Figure from Space Environment Topics [<http://www.swpc.noaa.gov/info/Iono.pdf>].

[4] Difficulties encountered by radio communications, GPS, and Differential GPS (DGPS) users are attributed to variations in electron density and therefore, TEC throughout the ionosphere. Radio communication is dependent upon electron density because the electromagnetic wave may experience a change in propagation direction due to gradients in electron density [Dabas, 2000]. According to the *AMS Policy Statement on Space Weather* [2008], commercial airlines' high-frequency (HF) radio signals are often degraded or lost as a result of space weather conditions. For example, during a strong radio blackout the electron density in the D-region increases greatly, which can render HF communications almost or completely unavailable and emergency communications used in disaster recovery on commercial flights over the polar regions useless [American Meteorological Society, 2008]. At any given GPS station, ionospheric TEC can change by tens or even hundreds of TEC units ( $1 \times 10^{16}$  electrons  $m^{-2}$ ), bringing about tens of meters of error in the given GPS position [Araujo-Pradere, 2005]. Even today, the ionosphere remains the largest error source of GPS navigation, which in turn could interfere with the Department of Defense's precision navigation and strike operations [Coster and Komjathy, 2008, American Meteorological Society, 2008]. DGPS users in North America experience detrimental effects during SED events [Skone and Coster, 2008]. Furthermore, the U.S. Department of Defense/Department of Transportation [2001] requires a

95% accuracy reading for marine horizontal positioning, safety, and navigation in inland waterways, which could be impossible for the Canadian and U.S. Coast Guard DGPS services to achieve [Skone and Coster, 2008]. Therefore, a technique to better determine electron densities and thus ionospheric TECs in real time, could lead to extensive improvements in our navigation and communication industries [Skone and Coster, 2008].

[5] Modeling the TEC in the ionosphere will better allow us to mitigate the aforementioned effects that this parameter has on our communication and navigation industries. In an effort to eventually predict the TEC along with ionospheric weather disturbances, both physics-based models and coupled models have been produced to combine different spatial domains [Scherliess *et al.*, 2006]. While theoretical/numerical models are fairly accurate at representing the observed climatological features in the ionosphere, these models generally are unsuccessful in replicating ionospheric weather [Scherliess *et al.*, 2006]. Presently, the most promising models for replicating ionospheric weather conditions are physics-based data-driven models that use a Kalman filter data assimilation techniques [Scherliess *et al.*, 2006].

[6] The Utah State University Global Assimilation of Ionospheric Measurements (USU-GAIM) Gauss-Markov Kalman Filter Model is a global data assimilation model that combines the physics based Ionospheric Forecast Model (IFM) with a suite of ionospheric observations (for more details see section 2) [Schunk *et al.*, 2004]. The Utah State University Gauss-Markov Kalman Filter (GMKF) was developed as a part of the Global Assimilation of Ionospheric Measurements (GAIM) in an effort sponsored by the Department of Defense (DoD) [Scherliess *et al.*, 2006]. The GMKF filter is used as a foundation for assimilating a distinct set of real-time (or near-real time) measurements [Scherliess *et al.*, 2006]. Furthermore, this model is currently used in operations at the Air Force Weather Agency (AFWA). For this study, global TEC as well as TEC over North America from the USU GAIM Gauss-Markov Kalman Filter Model will be of particular interest.

[7] The United States Total Electron Content (US-TEC) is a data-driven model that runs in real time (or near-real time) at the Space Weather Prediction Center (SWPC). US-TEC utilizes a sophisticated empirical model as background and a Kalman Filter data assimilation method, which is driven by a ground-based network of real time GPS stations [Fuller-Rowell *et al.*, 2006]. Recent validation efforts [Araujo-Pradere, *et al.*, 2007, Minter, *et al.* 2007] have showed that the accuracy of US-TEC is around 2.7 TECU for slant TEC, or about 2.00 TECU for vertical TEC. The US-TEC vertical TEC output over the continental United States (CONUS) will prove to be paramount for this research.

[8] The coupled thermosphere ionosphere plasmasphere electrodynamics (CTIPe) model is a physically based, non-linear, fully coupled thermosphere-ionosphere-plasmasphere model [<http://helios.swpc.noaa.gov/ctipe/CTIP.html>]. CTIPe includes four distinct components, which run concurrently and will be discussed with much greater depth in section 2. Also contained at <http://helios.swpc.noaa.gov/ctipe/CTIP.html>, is the evolution of the CTIPe model. Global TEC data from the CTIPe machine are used for comparison in this analysis.

[9] Providing adequate framework for this research are verification and validation studies on the abovementioned models, which include Scherliess *et al.*, [2006], Decker and McNamara,

2007, Araujo-Pradere et al., 2006, and Araujo-Pradere et al., [2007], Minter et al., [2006], Fuller-Rowell et al., [2006], and Fuller-Rowell et al., [1995], etc. In particular, this research focuses on statistical comparisons of global and CONUS (over the continental US) vertical TEC results from USU GAIM Gauss-Markov Kalman Filter Model, US-TEC, and CTIPe models. By calculating and later examining certain biases and root mean squared differences between the models, we will get a better sense of the discrepancies between models. Section 2 offers a more detailed description of each model used in this study. Section 3 discusses the computation of the statistical parameters and how the model output was plotted. Section 4 and 5 documents the biases and differences associated with each model comparison. Section 6 provides a summary and poses future research questions.

## 2. Models

### 2.1 The Utah State University Global Assimilation of Ionospheric Measurements (USU GAIM) Gauss-Markov Kalman Filter Model

[10] The Utah State University Gauss-Markov Kalman Filter (GMKF) Model was created as a part of the GAIM program [Schunk et al., 2004]. The GMKF is based on an ionospheric numerical model and a Kalman filter data assimilation algorithm [Scherliess et al., 2006]. Currently, the GMKF assimilates a number of different measurements including bottomside electron density ( $N_e$ ) profiles from a network of 100 Digisondes, nighttime line-of-sight ultraviolet (UV) radiances measured by satellites, line-of-sight TEC from as many as seventy GPS ground sites, TECs through occultations between various low-altitude satellites and between low- and high-altitude satellites, and in situ  $N_e$  from four Defense Meteorological Satellite Program (DMSP) satellites [Schunk et al., 2004, Scherliess et al., 2006]. Contained within the GMKF are plasma densities derived from the IFM, and it is these outputs that provide a background density field on which the perturbations measured by the GMKF are superimposed [Scherliess et al., 2006].

[11] The IFM is a global model of the ionosphere based on a numerical solution of the ion and electron continuity, momentum, and energy equations [Scherliess et al., 2006]. The IFM simulates these equations for heights from 90 km to 1400 km, which covers the E and F-regions of the ionosphere. The IFM accounts for all the important chemical and physical processes including field-aligned diffusion, electron thermal conduction, thermospheric winds, protonospheric exchange fluxes, energy-dependent chemical reactions, neutral composition changes, several ion production sources, cross-field electrodynamic drifts, a host of local heating and cooling processes, and the offset between the geomagnetic and geographic poles [Scherliess et al., 2006]. In an effort to simulate real-time operations, the model continuously runs and automatically produces 3-dimensional global electron density structure in fifteen-minute intervals as well as other auxiliary ionospheric parameters such as  $N_mF_2$ ,  $h_mF_2$ ,  $N_mE$ ,  $h_mE$ , slant and vertical TEC from 90 to 1400 km [Scherliess et al., 2006]. Displayed below (Figure 2a & 2b) are the IDL produced vertical TEC outputs plots from the USU GAIM GMKF Model.

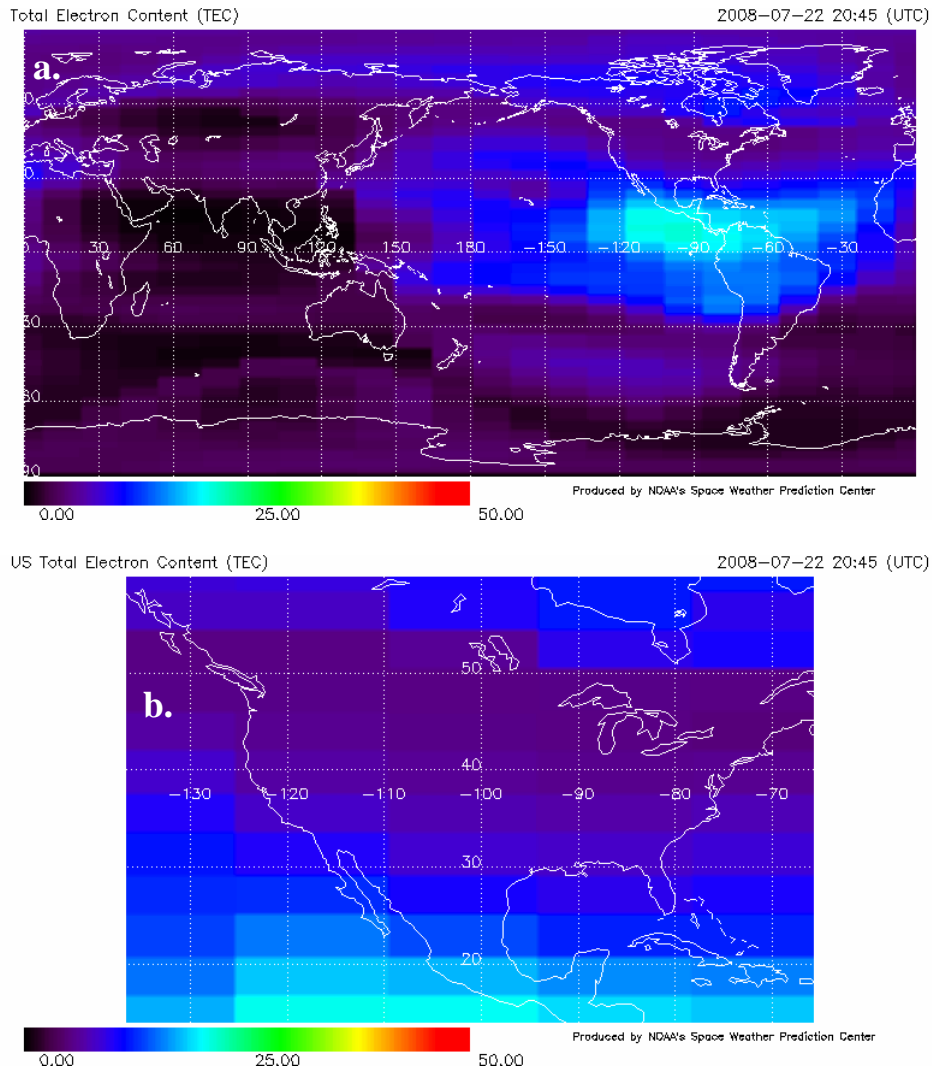


**Figure 2.** (a.) Sample map of the vertical global TEC for 20:45 UTC on 22 July 2008. (b.) Example plot of vertical TEC over CONUS for 20:45 UTC on 22 July 2008. The contour interval for both plots is given in TEC units.

## 2.2 The United States Total Electron Content (US-TEC) Model

[12] US-TEC was the first space weather product at the Space Weather Prediction Center (SWPC) to utilize a data assimilation scheme, and this product was first launched as a test operational product in November 2004 [Fuller-Rowell *et al.*, 2006], finally transitioning to a full operational model in June 2007 [Araujo-Pradere and Husler, 2007, Araujo-Pradere *et al.*, 2007, [http://www.swpc.noaa.gov/ustec/docs/USTEC\\_Doc.html](http://www.swpc.noaa.gov/ustec/docs/USTEC_Doc.html)]. As stated in section 1, US-TEC uses a Kalman filter to constantly update the ionospheric state every fifteen minutes, and as background the International Reference Ionosphere (IRI) model [Fuller-Rowell *et al.*, 2006]. The Maritime and Nationwide Differential GPS (M/NDGPS) real time network of stations operated by the US Coast Guard (USCG) acts as a principal data stream for the model [[http://www.swpc.noaa.gov/ustec/docs/USTEC\\_Doc.html](http://www.swpc.noaa.gov/ustec/docs/USTEC_Doc.html)]. Furthermore, GPS/Met network (meteorological application of GPS data) and the IGS (International GNSS Service) network

provide a secondary source of data for US-TEC [[http://www.swpc.noaa.gov/ustec/docs/USTEC\\_Doc.html](http://www.swpc.noaa.gov/ustec/docs/USTEC_Doc.html)]. Presently, there are about 80 CORS, 30 GPS/MET and 15 IGS stations utilized in the model [[http://www.swpc.noaa.gov/ustec/docs/USTEC\\_Doc.html](http://www.swpc.noaa.gov/ustec/docs/USTEC_Doc.html)]. Figure 3 displays the map of Vertical TEC over the CONUS up to 1400 km in TEC units for a given 15 minute interval. The US-TEC product also provides maps of estimated uncertainty, recent trends, and can provide current as well as past animations. New maps are usually available about thirteen minutes after a given interval, and are normally updated every fifteen minutes. The ASCII data files from US-TEC are available at <http://www.swpc.noaa.gov/ustec/index.html>.

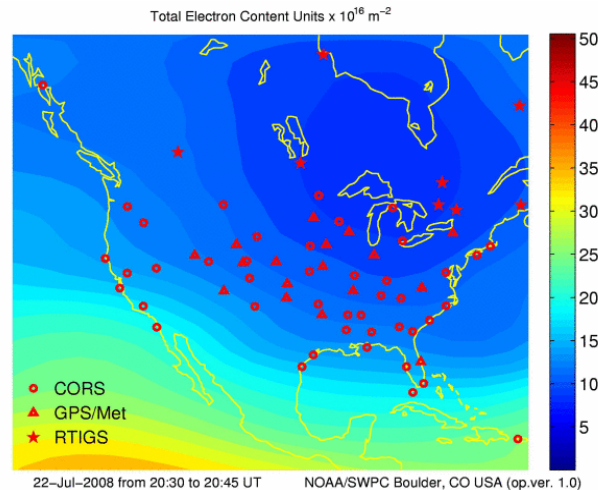


**Figure 3.** Sample map of the vertical TEC over CONUS for 20:45 UT on 22 July 2008. The symbols represent the different GPS sites used in the current assimilation cycle. Also the contour interval is given in TEC units. Data from ninety real-time GPS stations from the CORS, GPS/Met, and IGS networks are used for these calculations. This figure is from <http://www.swpc.noaa.gov/ustec/index.html>.

### 2.3 The Coupled Thermosphere Ionosphere Plasmasphere electrodynamics Model (CTIPe)

[13] The CTIPe Model is the name given to a physically based, global, three-dimensional, time-dependent, non-linear fully coupled thermosphere-ionosphere-plasmasphere model that unites four separate components [<http://helios.swpc.noaa.gov/ctipe/CTIP.html>, <http://www.issibern.ch/teams/effective-physics/CTIPeModel.pdf>]. The first component is a thermospheric model, which is originally described in *Fuller-Rowell and Rees* [1980], *Rees et al.* [1980], and in the Ph. D. thesis of *Fuller-Rowell* [1981]. A mid- and high-latitude dynamic ionospheric convention model described in *Quegan et al.*, [1982] was added as the second component. These first two components were originally coupled and became known as the Coupled Thermosphere-Ionosphere Model [*Fuller-Rowell et al.*, 1995]. Additional components were later added to CTIM; the first of these components was a plasmasphere and low latitude ionosphere [*Millward et al.*, 1996], which led to the Couple Thermosphere-Ionosphere-Plasmasphere Model. Lastly, the electrodynamics was solved using techniques from neutral dynamics and plasma components [<http://www.issibern.ch/teams/effective-physics/CTIPeModel.pdf>]. Currently, the CTIPe model is running at the SWPC in real-time (near real-time) producing plots of global TEC (Figure 4), electron density,  $N_mF_2$ ,  $h_mF_2$ , neutral

temperature, and O/N<sub>2</sub> Ratio up to altitudes of 500 to 600 km. All of these aforementioned plots are displayed at <http://helios.swpc.noaa.gov/ctipe>, along with some of the model inputs as well. Figure 4 presents an example of a vertical TEC output map from the CTIpe Model.

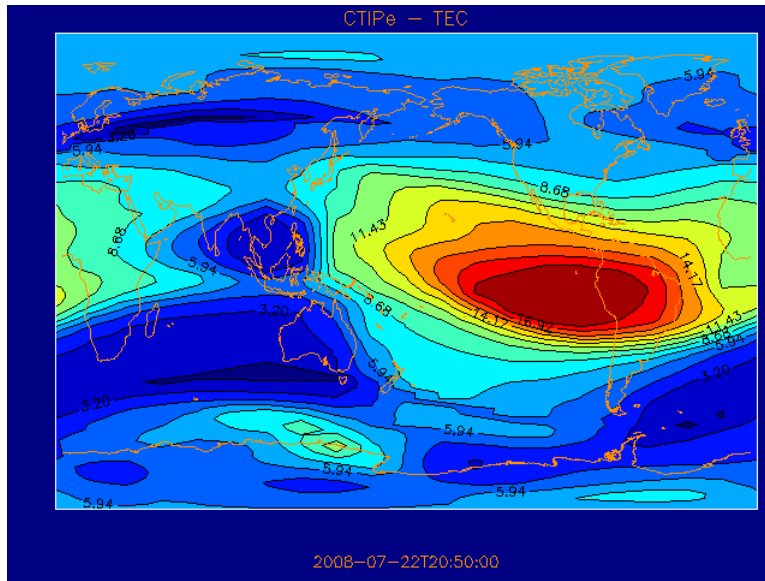


**Figure 4.** A sample plot of global TEC from the CTIpe model on 22 July 2008. The contours are plotted in TEC units. Figure from <http://helios.swpc.noaa.gov/ctipe/TEC.html>.

### 3. Model Outputs and Methodology

[14] The current study focuses on the vertical TEC output from the USU GAIM Gauss-Markov Kalman Filter, the USTEC, and CTIpe models. Since these models run in real-time (or near real-time), output files were readily available every fifteen minutes and for this research we focused on one or two weeks of daily fifteen minute data files in the month of July in 2008. During the data collection period we were experiencing a relatively quiescent sun, and therefore no extreme space weather events were observed. The Kp Index, which quantifies the intensity of the planetary geomagnetic activity, is displayed in the Appendix (Figure 5) over the entire period. With Kp Indices less than the threshold value ( $K_p = 5$ ) for the periods of interest, we can conclude that the analysis of these outputs was done under quiet conditions. For more information on Kp Indices see *Bother and Daglis* [2007] and <http://www.swpc.noaa.gov/info/Kindex.html>.

[15] In general, vertical TEC can be calculated by taking the line integral of the three-dimensional electron density ( $n_e$ ) profile as a function of height ( $h$ ) over the signal path from the GPS ground station to the satellite [*Bother and Daglis*, 2007],

(1)

$$TEC_v = \int n_e(h) dh,$$

where  $n_e$  is the electron density (electrons/cm<sup>3</sup>). Although, the above equation is solved in

each model, the USU GAIM Gauss Markov Kalman Filter model, the US-TEC model, and the CTIPe model reconstruct and or calculate the ionospheric vertical TEC differently. Since the CTIPe model is purely physics based model it solves the continuity and momentum equations for the plasma, and from there it represents the ionospheric state. The US-TEC model uses a background model completely driven by data to represent the state and then takes measurements of TEC. Subsequently, these measurements are then fit in through a data assimilation technique to give the best estimate of the ionospheric state. USU GAIM Gauss Markov Kalman Filter model uses as background a physics based model, which solves the background governing equations for the ionosphere. Then a set of observations is assimilated into the model and the state is modified to give the best representation of the current ionospheric state.

### 3.1 Methodology

[16] Creating global and CONUS vertical TEC maps from the USU GAIM Gauss-Markov Kalman Filter Model over the period of interest, allowed us to statistically and visually compare its output with the US-TEC and CTIPe models. The US-TEC and CTIPe plots were provided by Eduardo Araujo and Mihail Codrescu respectively, while the GAIM maps (both global and CONUS) were constructed using a modified IDL program, for which Michael Carpenter provided the base code. All the data collected throughout the study were plotted, however not every map is displayed. To facilitate the data collection process, three separate UNIX scripts were written (for the three separate models) to continuously provide real-time (or near real-time) data from each model, so that new maps could be plotted and current statistical parameters could be computed. For the statistical comparison of the vertical TEC output data was interpolated, since the resolution of each model was different. Given that we know the accuracy of the US-TEC vertical TEC outputs over CONUS, this model served as the basis for this statistical comparison. The following statistical comparisons are examined:

- USU GAIM Gauss-Markov Kalman Filter Model over CONUS vs. US-TEC Model
- CTIPe Model vs. US-TEC Model over CONUS
- Globally, the USU GAIM Gauss-Markov Kalman Filter vs. CTIPe Model

The US-TEC vs. GAIM comparison started with data from 2 July 2008 to 15 July 2008. The US-TEC vs. CTIPe and GAIM vs. CTIPe comparisons began with data from 16 July 2008 to 22 July 2008.

[17] The first statistical parameter computed for the above comparison scenarios was the average difference. The average vertical TEC was solved for every fifteen minute interpolated output file and to obtain the average difference we subtracted the average vertical TEC between

the two output files from the models of interest at the same instance in time for each one of our above comparison scenarios. These are plotted as a function of time over the period of interest and give us a sense of the consistent differences between the models. The average difference provides us with a method of monitoring model biases.

[18] The root square difference presents a sufficient statistical technique for measuring vertical TEC differences between corresponding output points in each one of our interpolated fifteen-minute data files. The root mean square difference always returns positive values of vertical TEC, which will tell us absolutely how different the output points are. The root mean square difference can be represented in general as:

$$\theta_1 = \begin{matrix} x_{1,1} \\ x_{1,2} \\ x_{1,3} \\ \vdots \\ x_{1,n} \end{matrix} \quad \text{and} \quad \theta_2 = \begin{matrix} x_{2,1} \\ x_{2,2} \\ x_{2,3} \\ \vdots \\ x_{2,n} \end{matrix}$$

where  $\theta_1$  and  $\theta_2$  are two data arrays and the first index represents the model while the second shows the grid point.

The formula then becomes:

$$RMS\ Difference(\theta_1, \theta_2) = \sqrt{\frac{\sum_{i=1}^n (x_{1,i} - x_{2,i})^2}{n}} \quad (2)$$

[19] This is done as function of time for the three comparison scenarios. Small values of RMS difference occur when the predicted values of vertical TEC from each model are relatively close. Large RMS difference values arise when the forecasted values of vertical TEC from the two models are comparatively different.

## 4. Average Difference Validation

### 4.1 USU-GAIM Gauss-Markov Kalman Filter Model vs. US-TEC Model

[20] The average difference is shown for the GAIM vs. US-TEC comparison in Figure 5. Both weeks exhibit a robust diurnal variation; furthermore, this diurnal variation is consistent everyday and is strikingly similar from week-to-week. During week 1 (Figure 5a) the mean average difference was 5.00 TECU, with the maximum average difference (7.96 TECU) occurring on the 5 July 2008 at 2:00 UTC and the minimum average difference (1.63 TECU) observed on the 6 July 2008 at 12:00 UTC. During week 2 (Figure 5b) we recorded a mean average difference of 4.65 TECU, with maximum average difference of 8.23 TECU on 9 July 2008 at 1:45 UTC, while on 12 July 2008 at 12:00 UTC the minimum average difference was measured to be 1.38 TECU. The average difference was computed by subtracting the average GAIM vertical TEC value from the average US-TEC vertical TEC output, meaning there is a US-TEC model bias to predict higher vertical TEC values than the GAIM model. The mean bias between the two weeks is 4.825 TECU; also the relative error between the two models was 81.8%.

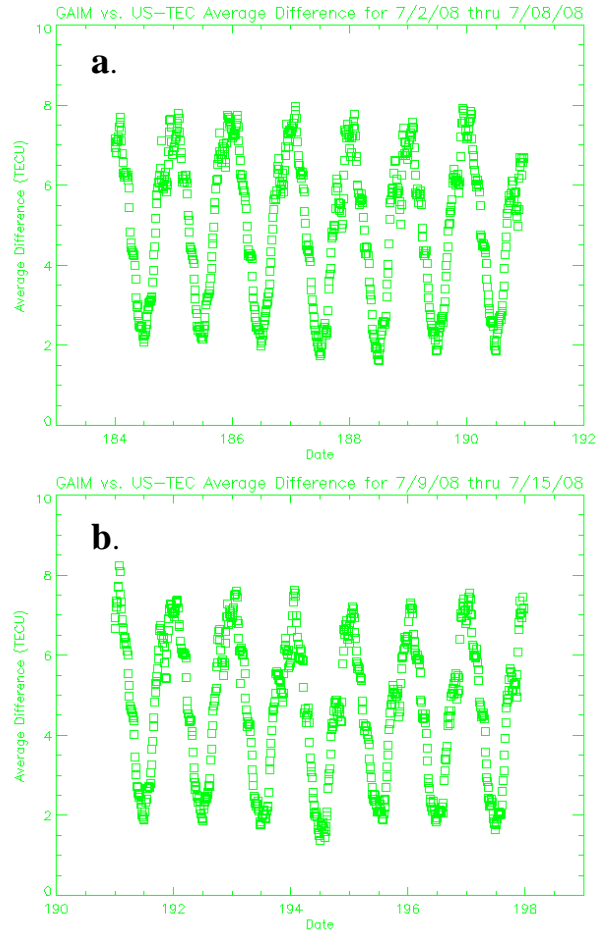


**Figure 5.** Average difference plots for GAIM vs. US-TEC (a) 2 July 2008 at 0:00 UTC to 8 July 2008 at 23:45 UTC and for (b) 9 July 2008 at 0:00 UTC and ends on 15 July 2008 at 23:45 UTC.

[21] For the first two comparisons we are taking the US-TEC model to be the best representation of the ionospheric state because we know the errors and uncertainties associated with this model [Araujo-Pradere and Husler, 2007, Minter, et al. 2007]. The majority of the US-TEC validation has been done exclusively over the CONUS (where the model has a data input source); however this validation has not been extended to include the edges of the output plots. Below we have plotted the GAIM (Figure 6a) and US-TEC (Figure 6b) vertical TEC output maps at the time when we measured the greatest average difference (8.23 TECU) between the models during our entire two-week period. As can be seen from Figure 6, the US-TEC model is displaying values of about 30 TECU in the southwest corner of the plot, while the GAIM plot shows a maximum in that same region only its maximum vertical TEC was about 20 TECU. The southwest corners of both plots display the largest values, therefore dominating the average difference comparison. Due to the lack of data input in the US-TEC model below 25° N, we limited our comparison region to the regions covered by data (e.g. - 25° N to 60° N instead of 12° N to 60° N).

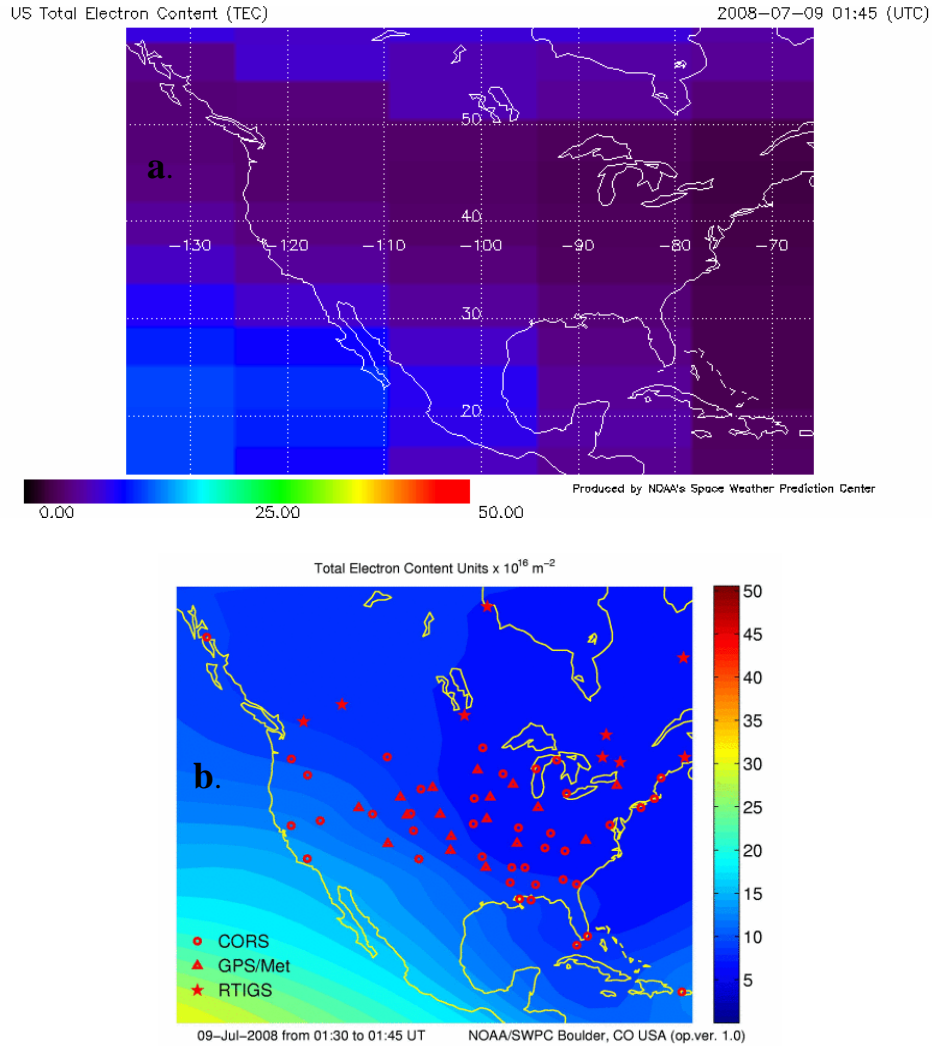


**Figure 6.** (a) Vertical TEC from the GAIM model over CONUS for 1:45 UTC on 9 July 2008. The contour interval for both plots is given in TECU units. (b) Vertical TEC output map from the US-TEC model over CONUS for 1:45 UT on 9 July 2008.

[22] The limited region average difference for the two weeks is displayed in Figure 7. These average difference plots display the same robust diurnal variation feature as those for the non-limited case. However, the y-axis scale on these limited coverage plots only extend to 6 TECU whereas the non-limited coverage y-axis scale reaches to 8 TECU for the first week and 10 TECU for the second week. During week 1 the mean average difference was 3.21 TECU, with a maximum average difference of 5.65 TECU, which took place at 2:00 UTC on 8 July 2008, and a minimum average difference of 0.77 TECU occurring at 12:00 UTC on 6 July 2008. In week 2 the minimum average difference was calculated to be 0.53 TECU, which occurred at 12:00 UTC on 12 July 2008 and a maximum average difference of 5.68 taking place on 9 July 2008 at 2:00 UTC. The mean average difference for week 2 was calculated to be 2.88 TECU. Consequently, the bias for the US-TEC model to predict higher average values of vertical TEC when compared to the GAIM model has shrunk to 3.045 TECU. Additionally, our relative error between the two was reduced to 57.1%; thus, by limiting our coverage area the models start to converge towards predicting similar vertical TEC values.

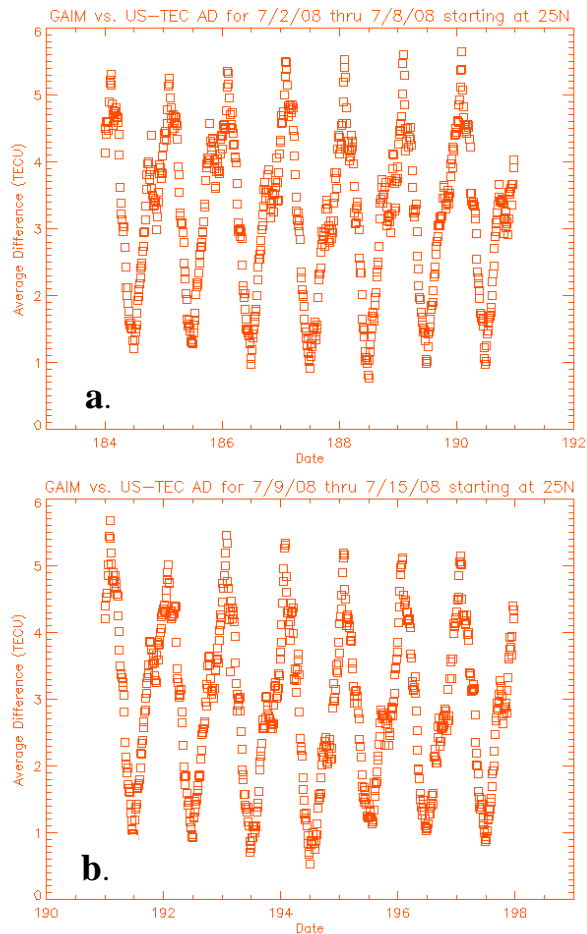


**Figure 7.** Average difference plots starting at 25° N for GAIM vs. US-TEC (a) 2 July 2008 at 0:00 UTC to 8 July 2008 at 23:45 UTC and for (b) 9 July 2008 at 0:00 UTC and ends on 15 July 2008 at 23:45 UTC.

#### 4.2 CTIPe Model vs. US-TEC Model

[23] The CTIPe vs. US-TEC average difference (Figure 8) was computed the same way, as the previous comparison except the period of interest is different. Once again the diurnal variation is easily observed with a higher average difference experienced in the afternoon/evening hours and a lower average difference seen in the morning hours. This diurnal variation is consistent during the entire week. The mean average difference over this week long period was 5.32 TECU, with a maximum average difference calculated on 22 July 2008 at 21:15 UTC of 10.54 TECU and a minimum average difference of 1.51 TECU observed on 21 July 2008 at 11:15 UTC. Additionally, very slight increase in the local maximum average difference throughout the week, with the exception of the 19 July 2008 maximum average difference. The positive average difference calculations reveals a US-TEC bias to predict higher average values of vertical TEC in comparison to the CTIPe model. The bias in this comparison is slightly higher than that of the model bias in the previous comparison. Furthermore, the relative error between the models was calculated to be 79.9%.

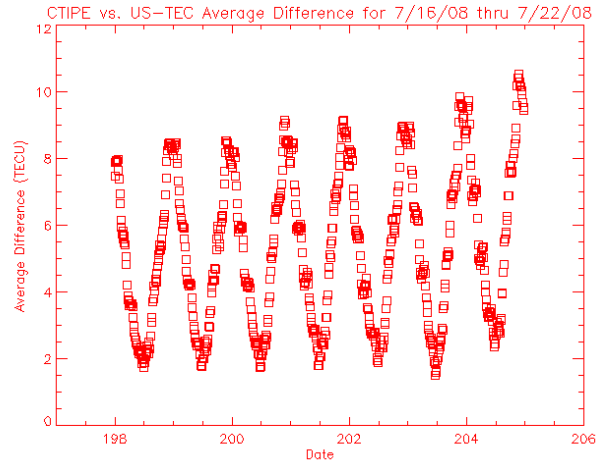


**Figure 8.** Average difference plot for CTIPe vs. US-TEC starting on 16 July 2008 at 0:00 UTC and ending on 22 July 2008 at 23:45 UTC.

[24] Given that CTIPe is a global model we will extend our limited coverage case for this particular comparison as well. As was previously stated we limit our region to start at 25° N and extend to 60° N instead of 12° N to 60° N. The mean average difference over our week period has now dropped to 3.96 TECU showing the US-TEC model still tends to predict higher average vertical TEC values when compared to the CTIPe model. Also the relative error between the two models has slightly decreased to 75.2%. A maximum average difference of 7.34 TECU occurred at 1:00 UTC on 22 July 2008 and a minimum average difference of 1.32 TECU was calculated on 21 July 2008 at 11:15 UTC. The consistent diurnal variation in the average difference is still the dominant characteristic. Additionally, the y-axis scale decreased from 12 TECU to 8 TECU when we limited our comparison region.

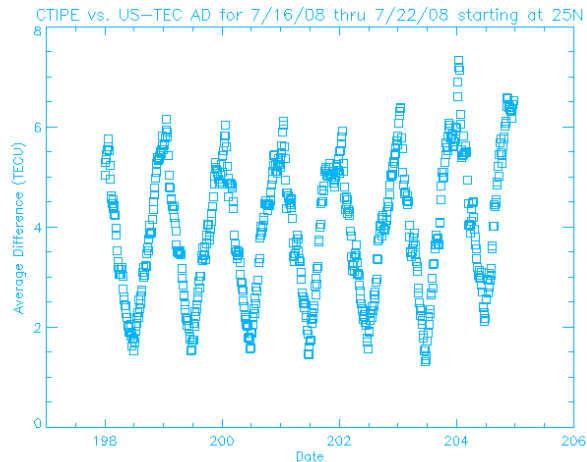


**Figure 9.** Average difference plot starting at 25° N for CTIPe vs. US-TEC on 16 July 2008 at 0:00 UTC to 22 July 2008 at 23:45 UTC.

#### 4.3 -GAIM Gauss-Markov Kalman Filter vs. CTIPe Model

[25] The final average difference comparison between GAIM vs. CTIPe is displayed in Figure 10. The average difference between the predicted global vertical TEC values between

these two models is much smaller than that of the previous two comparisons discussed in Sections 4.1-4.2. Once more diurnal variability is observed, however this diurnal dependence is more variable for this particular situation. A mean average difference of 1.64 TECU, with a maximum average difference of 2.61 TECU calculated on 21 July 2008 at 17:30 UTC, and a minimum average difference of 0.57 TECU of was experienced on 16 July 2008 at 0:30 UTC. With positive average difference calculations, globally, the average vertical TEC predicted by the CTIPe model is slightly higher than that of the GAIM model. However, this bias is not as great as the aforementioned comparisons over the CONUS and the relative error is noticeably smaller (22.4%). Figure 9 also shows that this scenario is unique in the sense that the smallest average differences are observed in the afternoon/evening and the largest average differences occur during the morning hours.

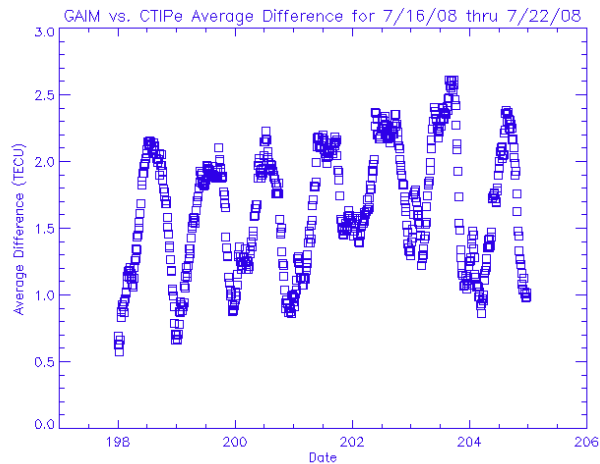


**Figure 10.** Global average difference plot for GAIM vs. CTIPe from 16 July 2008 at 0:00 UTC to 22 July 2008 at 23:45 UTC.

## 5. RMS Difference Validation

[26] Subsequent to quantifying the differences between the models, some further research was required to examine where the greatest differences were being experienced. Figure 11 shows the RMS difference over our two-week period (2 July 2008 through 15 July 2008) for the GAIM vs. US-TEC comparison. In general there are considerably higher RMS differences between corresponding data points in the southern half of the plot as compared to the northern half. The largest RMS differences are seen in the southwest part of the CONUS. The region of largest RMS Difference corresponds to poor or no data coverage from the US-TEC model. This indicates perhaps that the IRI model used as a background in the data assimilation scheme is having difficulty reconstructing the vertical TEC in the regions with minimal or no data coverage. Additionally, in the northeast portion of the map the models agree and there is a small RMS difference calculated here over our two-week period.

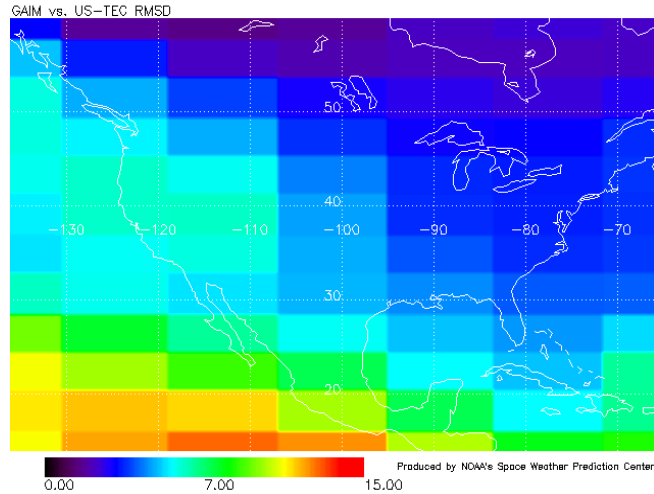


**Figure 11.** RMS difference map for GAIM vs. US-TEC from 2 July 2008 to 15 July 2008. The contours are plotted in TECU.

[27] Below, Figure 12 is strikingly similar to Figure 11 however; Figure 12 displays the output map from the CTIPe vs. US-TEC model comparison. Another characteristic that is analogous to both figures in the structure of the RMS difference. Yet again we observed smaller RMS difference values located in the northeast portion of the graph and larger values of RMS difference in the southwest region of the map. Also, with the largest RMS difference observed to be in the southern parts of the CONUS, this reinforces that the maximum differences between the models occur where there is a lack of real-time vertical TEC data being assimilated into the US-TEC model. Moreover, Figure 12 strengthens our above statement that in the northeastern areas of the CONUS the models are in reasonable accord.

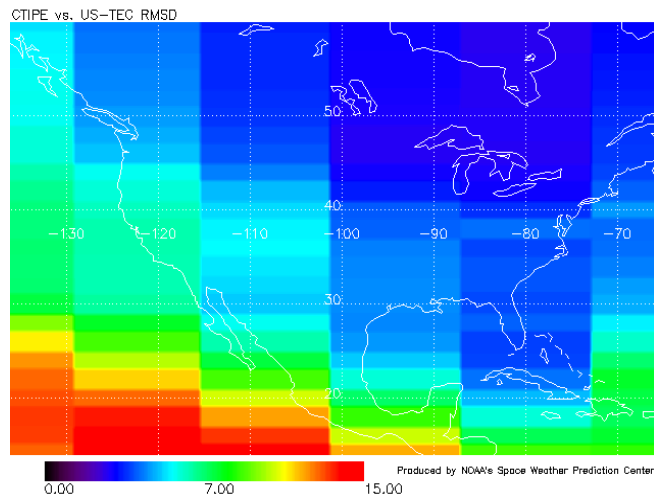


**Figure 12.** RMS difference plot for CTIPe vs. US-TEC from 16 July 2008 to 22 July 2008. The contours are plotted in TECU.

[28] Figure 13 shows the global GAIM vs. CTIPe RMS difference. Notice that the scale has shifted from a maximum of 15 TECU in the preceding maps to 10 TECU in this figure. The

largest discrepancies between the models are observed in the tropical regions of the globe. The smallest values of RMS difference are calculated in the mid-latitudes, where the physics of the ionosphere are better known. Additionally, the ionospheric dynamics exhibited at mid-latitudes in the ionosphere are not nearly as intense when compared to the equatorial ionosphere. Also, notice that the polar regions in the northern hemisphere have RMS difference values that are about a factor of two smaller than the RMS difference at high latitudes in the southern hemisphere. We believe this is due to the lack of data coverage at high-latitudes in the southern hemisphere relative to the northern hemisphere in the GAIM model.

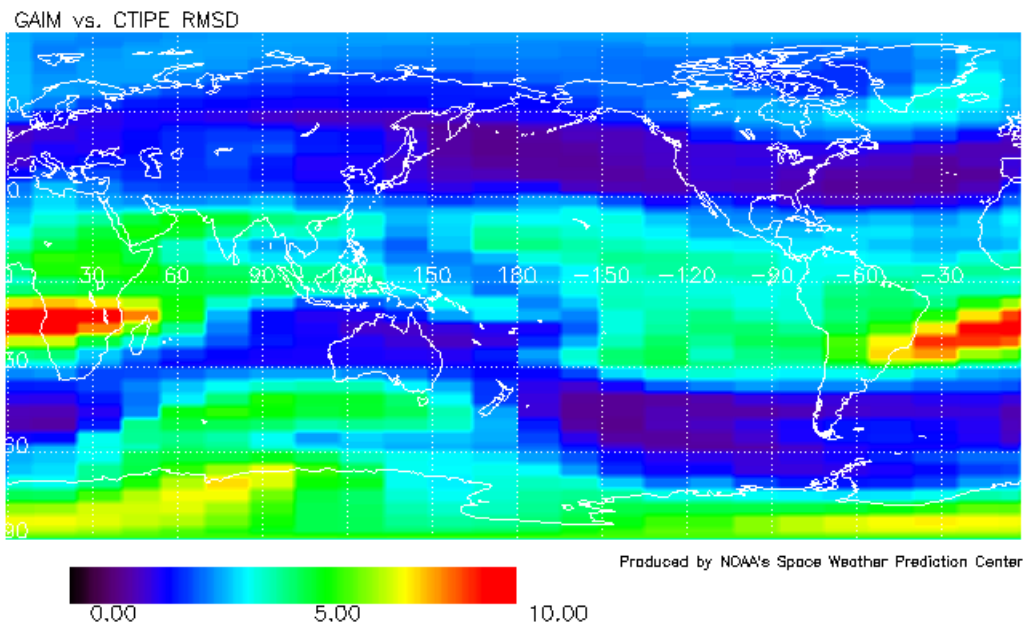


**Figure 13.** Global RMS difference map for GAIM vs. CTIPe from 16 July 2008 to 22 July 2008. The contours are plotted in TECU.

## 6. Summary and Conclusions

[29] Vertical TEC, especially in periods of high solar and geomagnetic activity can have detrimental effects on both navigation and communication systems. Recent studies have shown that by accurately modeling vertical TEC we can reduce some the difficulties experienced by radio communications, GPS, and DGPS users. By comparing three different ionospheric models that are running in real-time (or near real-time) and documenting certain biases and uncertainties associated with each one of the models, we hope to further alleviate some of these adverse effects.

[30] Computing the average differences allowed us to observe consistent differences between the models. The GAIM vs. US-TEC comparison provided evidence that the US-TEC model generally predicts higher average values of vertical TEC. Once the area was restricted to exclude the part of the US-TEC model that had poor or no data coverage the GAIM and US-TEC models were in better agreement. Users of these models should exercise caution when they are looking at regions where little to no data is being assimilated into the models. The CTIPe vs. US-TEC comparison further reinforced the above claim showing that when the observed regions were

limited the models were in better agreement. On a global scale, the GAIM vs. CTIPe are in reasonable agreement showing a mean average difference of 1.64 TECU over our data collection period.

[31] By calculating the RMS differences between the models, we were able to determine geographically where the models predicted vertical TEC values diverged. Both the GAIM vs. US-TEC and CTIPe vs. US-TEC comparisons showed that the largest differences between the two models were calculated in the southwest part of the CONUS. Additionally, both these comparisons showed that the vertical TEC values converged as we approached the northeastern region of the CONUS. The above RMS difference results provided further evidence that the forecasted vertical TEC values diverged in the areas where the US-TEC model has poor data coverage. Globally, the GAIM and CTIPe models are in reasonable agreement, with the exception of a small area in the tropics and in the high-latitudes of the southern hemisphere.

[32] This research has presented the initial comparison between the GAIM, CTIPe, and US-TEC models. Nevertheless, there are additional areas that warrant a greater in-depth analysis so that we can better quantify the difference between the models and discover the underlying causes of these discrepancies. Our analysis of reducing the coverage area to show that the agreement between the models improves can be extended to decrease the coverage region even further to see if the models continue to converge. Furthermore, determining how these statistics would change during a period of higher solar activity and therefore higher geomagnetic activity would provide us with a more holistic synopsis of these model differences. Collecting data over a longer time scale would prove essential in refining the above findings. In summary, the culminating goal of this research is to better equip forecasters with a sense of where and when the different models are proficient at predicting ionospheric weather.

## **7. Acknowledgements**

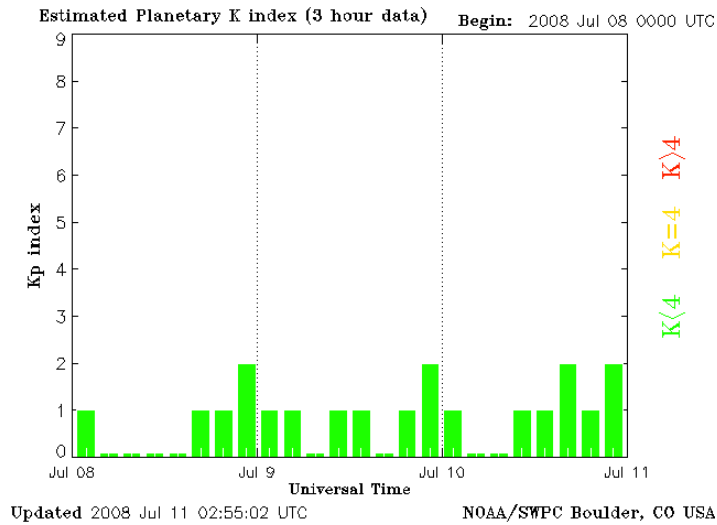
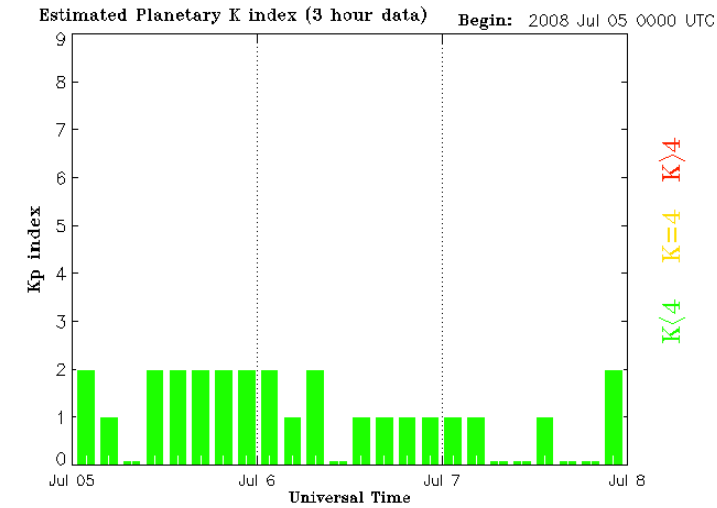
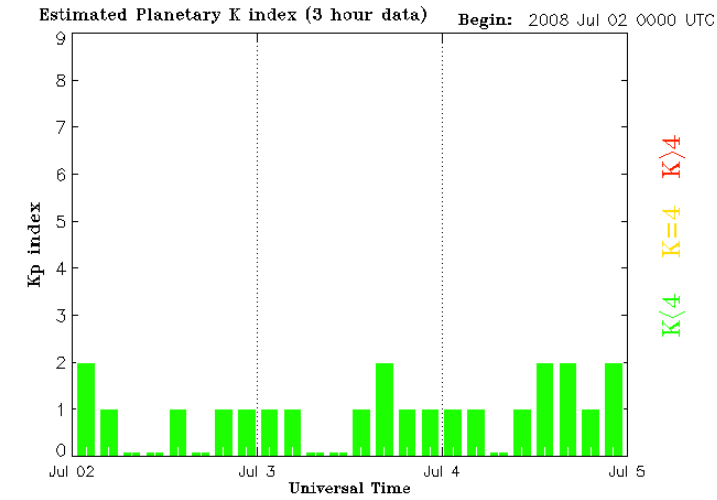
[33] Thank you to all of the SOARS® Staff and Protégés, the RESESS® Staff and Protégés, and each scientist from the National Oceanic and Atmospheric Administration/Earth System Research Laboratory/Space Weather Prediction Center that contributed to this research. A special thanks to my scientific mentors Mihail Codrescu and Jennifer Gannon and my writing and communications mentor Marijke Unger for all of your hard work and devotion in making this summer a successful one. Additionally, special thanks goes out to Michael Carpenter, Bill Murtaugh, Rob Craver, Chris Balch, Eduardo Araujo-Pradere, Tim Fuller-Rowell, the Air Force Weather Agency, Russ Henson, Kelvin Fedrick, Michael Husler, Robert Masten, and Paul Johnston for their assistance on this project.

## **References:**

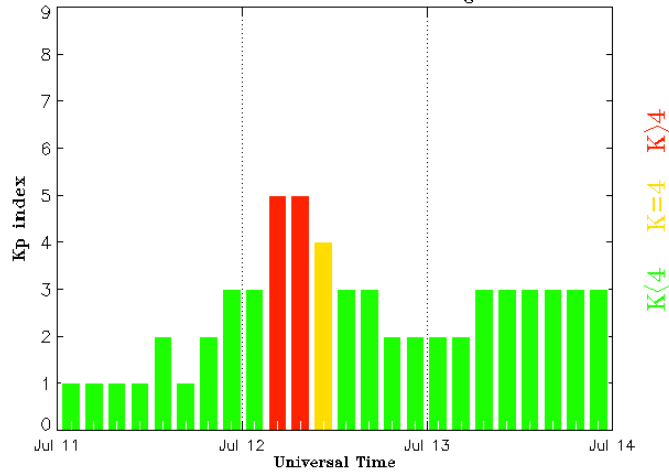
- American Meteorological Society (2008), SPACE WEATHER A Policy Statement of the American Meteorological Society, *Bulletin of the American Meteorological Society*, 89, (6), 16-18.
- American Meteorological Society (2000), *Glossary of Meteorology*, 2, 855 pp., American Meteorological Society, Boston, MA.
- Araujo-Pradere, E. A., T. J. Fuller-Rowell, and M. V. Codrescu, STORM: An empirical storm-time ionospheric correction model, 1, Model description, *Radio Sci.*, 37(5), 1070, doi:10.1029/2001RS002467, 2002.
- Araujo-Pradere, E. A., and T. J. Fuller-Rowell, STORM: An empirical storm-time ionospheric correction model, 2, Validation, *Radio Sci.*, 37(5), 1071, doi:10.1029/2002RS002620, 2002.
- Araujo-Pradere, E. A. (2005), GPS-derived total electron content response for the Bastille Day magnetic storm of 2000 at a low mid-latitude station, *Geofisica Internacional*, 5, 211-218.
- Araujo-Pradere, E.A., M. Husler. US-Total Electron Content, Integrated Documentation. Technical Report, Space Environment Center. National Oceanic and Atmospheric Administration. USA. 2007.
- Araujo-Pradere, E. A., T. J. Fuller-Rowell, P. S. J. Spencer, and C. F. Minter (2007), Differential validation of the US-TEC model, *Radio Sci.*, 42, RS3016, doi:10.1029/2006RS003459.
- Bothmer, V. and I. A. Daglis (2007), *Space Weather: Physics and Effects*, 213, 315-318, 438 pp., Praxis Publishing Ltd., Chichester, UK.
- Coster, A. and A. Komjathy (2008), Space Weather and the Global Positioning System, *Space Weather*, 6, S06D04, doi: 10.1029/2008SW000400.f.
- Dabas, S. R. (2000), Ionosphere and its Influence on Radio Communication, *Journal of Science Education*, 5, 28 – 43.
- Davies, N. C., M. J. Maundrell, P. C. Arthur, P. S. Cannon, R. C. Bagwell, J. Cox (1997), Modern aircraft HF communications into the 21<sup>st</sup> Century, *IEE Colloquium on Air-To-Ground Communications (1997/397)*, 2/1 – 2/9.
- Decker, D. T., and L. F. McNamara (2007), Validation of ionospheric weather predicted by Global Assimilation of Ionospheric Measurements (GAIM) models, *Radio Sci.*, 42, RS4017, doi:10.1029/2007RS003632.
- Fuller-Rowell, T. J., Three-dimensional, time-dependent model of the thermosphere, Ph.D. thesis, Univ. College London, London, England, 1981.

- Fuller-Rowell, T.J., and D. Rees, A three-dimensional time dependent global model of the thermosphere, *J. Atmos. Sci.*, 37, 2545, 1980.
- Fuller-Rowell, T., D. Rees, S. Quegan, R.J. Moffett, M.V. Codrescu, and G.H. Millward (1995), A Coupled thermosphere-ionosphere model (CTIM), *STEP Handbook*.
- Fuller-Rowell, T., E. Araujo-Pradere, C. Minter, M. Codrescu, P. Spencer, D. Robertson, and A. R. Jacobson (2006), US-TEC: A new data assimilation product from the Space Environment Center characterizing the ionospheric total electron content using real-time GPS data, *Radio Sci.*, 41, RS6003, doi:10.1029/2005RS003393.
- Goodman, J., M. and J. Aarons (1990), Ionospheric Effects on Modern Electronic Systems, *Proceedings of the IEEE*, 78, 512 – 528.
- Millward, G. H., H. Rishbeth, T. J. Fuller-Rowell, A. D. Aylward, S. Quegan, and R. J. Moffett (1996), Ionospheric  $F_2$  layer seasonal and semiannual variations, *J. Geophys. Res.*, 101(A3), 5149–5156.
- Minter, C. F., D. S. Robertson, P. S. J. Spencer, A. R. Jacobson, T. J. Fuller-Rowell, E. A. Araujo-Pradere, and R. W. Moses (2007), A comparison of Magic and FORTE ionosphere measurements, *Radio Sci.*, 42, RS3026, doi:10.1029/2006RS003460.
- Quegan, S., G. J. Bailey, R. J. Moffett, R. A. Heelis, T. J. Fuller Rowell, D. Rees, and R. W. Spiro, A theoretical study of the distribution of ionization in the high-latitude ionosphere and the plasmasphere: first results on the mid-latitude trough and the light ion trough, *J. Atmos. Terr. Phys.*, 44, 619, 1982.
- Rees, D., T. J. Fuller-Rowell, and R. W. Smith, Measurements of mid latitude thermospheric winds by rocket and ground-based techniques and their interpretation using a three-dimensional, time-dependent dynamic model, *Planet. Space Sci.*, 28, 919, 1980.
- Scherliess, L., R. W. Schunk, J. J. Sojka, D. C. Thompson, and L. Zhu (2006), Utah State University Global Assimilation of Ionospheric Measurements Gauss-Markov Kalman filter model of the ionosphere: Model description and validation, *J. Geophys. Res.*, 111, A11315, doi: 10.1029/2006JA011712.
- Schunk, R. W., et al. (2004), Global Assimilation of Ionospheric Measurements (GAIM), *Radio Sci.*, 39, RS1S02, doi:10.1029/2002RS002794.
- Skone, S., and A. Coster (2008), Potential for issuing ionospheric warnings to Canadian users of marine DGPS, *Space Weather*, 6, S04D03, doi:10.1029/2007SW000336.

## 8. Appendix

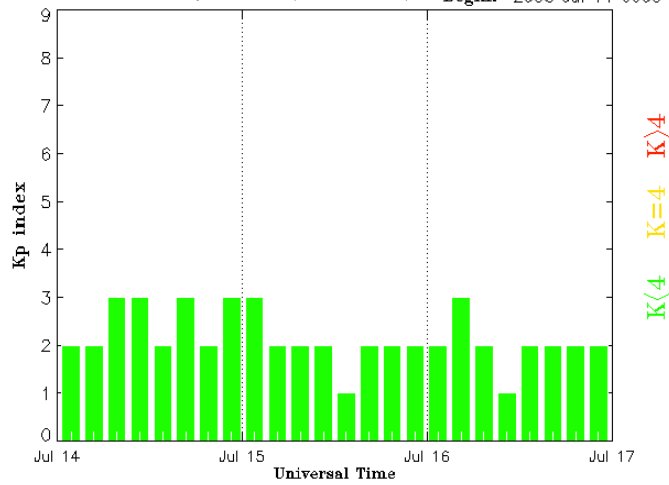


Estimated Planetary K index (3 hour data) Begin: 2008 Jul 11 0000 UTC



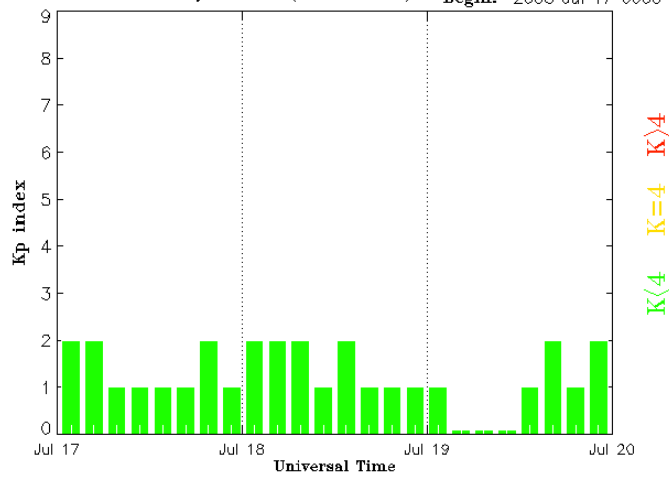
Updated 2008 Jul 14 02:55:02 UTC NOAA/SWPC Boulder, CO USA

Estimated Planetary K index (3 hour data) Begin: 2008 Jul 14 0000 UTC



Updated 2008 Jul 17 02:55:02 UTC NOAA/SWPC Boulder, CO USA

Estimated Planetary K index (3 hour data) Begin: 2008 Jul 17 0000 UTC



Updated 2008 Jul 20 02:55:02 UTC NOAA/SWPC Boulder, CO USA

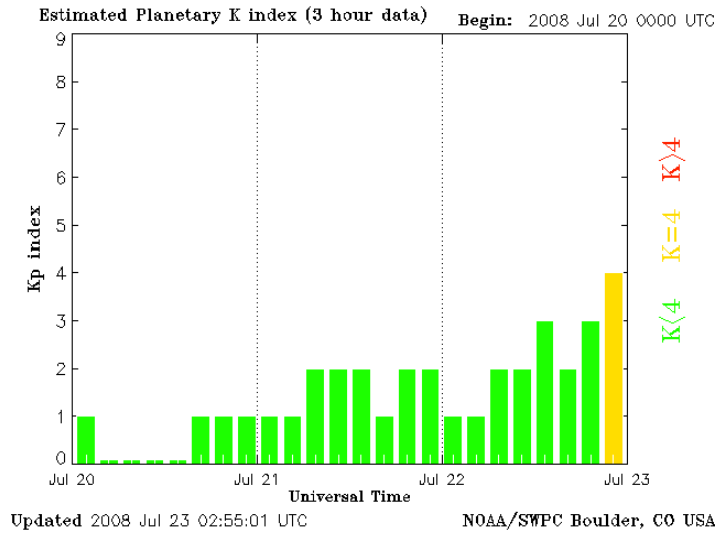


**Figure 5.** 3-day Satellite Environment Plots of estimated planetary Kp indices from 2 July 2008 to 22 July 2008. Plots can be accessed at <http://www.swpc.noaa.gov/ftpmenu/plots/satenv.html>.